

**Supplementary Table 1: Genotype description of H3.3 and H3 K9R mutants.**

Nomenclature <sup>a</sup>	Genotype
<i>WT</i> <sup>b</sup>	$\frac{+}{+}; \frac{+}{+}$
<i>H3.3B</i> <sup>K9R</sup>	$\frac{H3.3B^{K9R}}{H3.3B^{K9R}}; \frac{+}{+}$
<i>H3.3A</i> <sup>Null</sup>	$\frac{+}{+}; \frac{H3.3A^{2x1}}{Df(2L)BSC110}$
<i>H3.3</i> <sup>K9R</sup>	$\frac{H3.3B^{K9R}}{H3.3B^{K9R}}; \frac{H3.3A^{2x1}}{Df(2L)BSC110}$
<i>H3</i> <sup>HWT</sup>	$\frac{+}{+}; \frac{His\Delta, twiGal4}{His\Delta, UAS YFP}; \frac{12x H3^{HWT}}{+}$
<i>H3</i> <sup>K9R</sup>	$\frac{+}{+}; \frac{His\Delta, twiGal4}{His\Delta, UAS YFP}; \frac{12x H3^{K9R}}{+}$
<i>H3.3</i> <sup>K9R</sup> <i>H3</i> <sup>HWT</sup>	$\frac{H3.3B^{K9R}}{H3.3B^{K9R}}; \frac{H3.3A^{2x1}, His\Delta, twiGal4}{H3.3A^{2x1}, His\Delta, UAS YFP}; \frac{12x H3^{HWT}}{+}$
<i>H3.3</i> <sup>K9R</sup> <i>H3</i> <sup>K9R</sup>	$\frac{H3.3B^{K9R}}{H3.3B^{K9R}}; \frac{H3.3A^{2x1}, His\Delta, twiGal4}{H3.3A^{2x1}, His\Delta, UAS YFP}; \frac{12x H3^{K9R}}{+}$

<sup>a</sup> Top four rows indicate genotypes used for variant H3.3<sup>K9R</sup> studies. Bottom four rows indicate genotypes used for combined variant and canonical H3.3<sup>K9R</sup> H3<sup>K9R</sup> experiments.

<sup>b</sup> Wild-type chromosomes represented with “+”.

A

$$\frac{H3.3B^{K9R} (1)}{H3.3B^{K9R} (1)}; \frac{CyO, twiGFP}{If} \times \frac{H3.3B^{K9R} (1)}{Y}; \frac{H3.3A^{2x1}}{CyO} \quad \left| \quad \frac{H3.3B^{K9R} (2)}{H3.3B^{K9R} (2)}; \frac{CyO, twiGFP}{If} \times \frac{+}{Y}; \frac{Df(2L)BSC110}{CyO}$$



$$\frac{H3.3B^{K9R} (1)}{H3.3B^{K9R} (1)}; \frac{H3.3A^{2x1}}{CyO, twiGFP} \times \frac{H3.3B^{K9R} (2)}{Y}; \frac{Df(2L)BSC110}{CyO, twiGFP}$$



$$\frac{H3.3B^{K9R} (1)}{H3.3B^{K9R} (2)}; \frac{H3.3A^{2x1}}{Df(2L)BSC110}$$

$WT = \frac{+}{+}; \frac{+}{+}$
$H3.3B^{K9R} = \frac{H3.3B^{K9R}}{H3.3B^{K9R}}; \frac{+}{+}$
$H3.3A^{Null} = \frac{+}{+}; \frac{H3.3A^{2x1}}{Df(2L)BSC110}$
$H3.3^{K9R} = \frac{H3.3B^{K9R}}{H3.3B^{K9R}}; \frac{H3.3A^{2x1}}{Df(2L)BSC110}$

B

$$\frac{H3.3B^{K9R} (2)}{H3.3B^{K9R} (2)}; \frac{+}{+}; \frac{+}{+} \times \frac{+}{Y}; \frac{H3.3A^{2x1}, His\Delta, UAS2xYFP}{CyO}; \frac{12x H3^{HWT} \text{ or } 12x H3^{K9R}}{12x H3^{HWT} \text{ or } 12x H3^{K9R}}$$



$$\frac{H3.3B^{K9R} (2)}{Y}; \frac{H3.3A^{2x1}, His\Delta, UAS2xYFP}{+}; \frac{12x H3^{HWT} \text{ or } 12x H3^{K9R}}{+} \times \frac{H3.3B^{K9R} (1)}{H3.3B^{K9R} (1)}; \frac{H3.3A^{2x1}, His\Delta, twiGal4}{CyO}; \frac{+}{+}$$

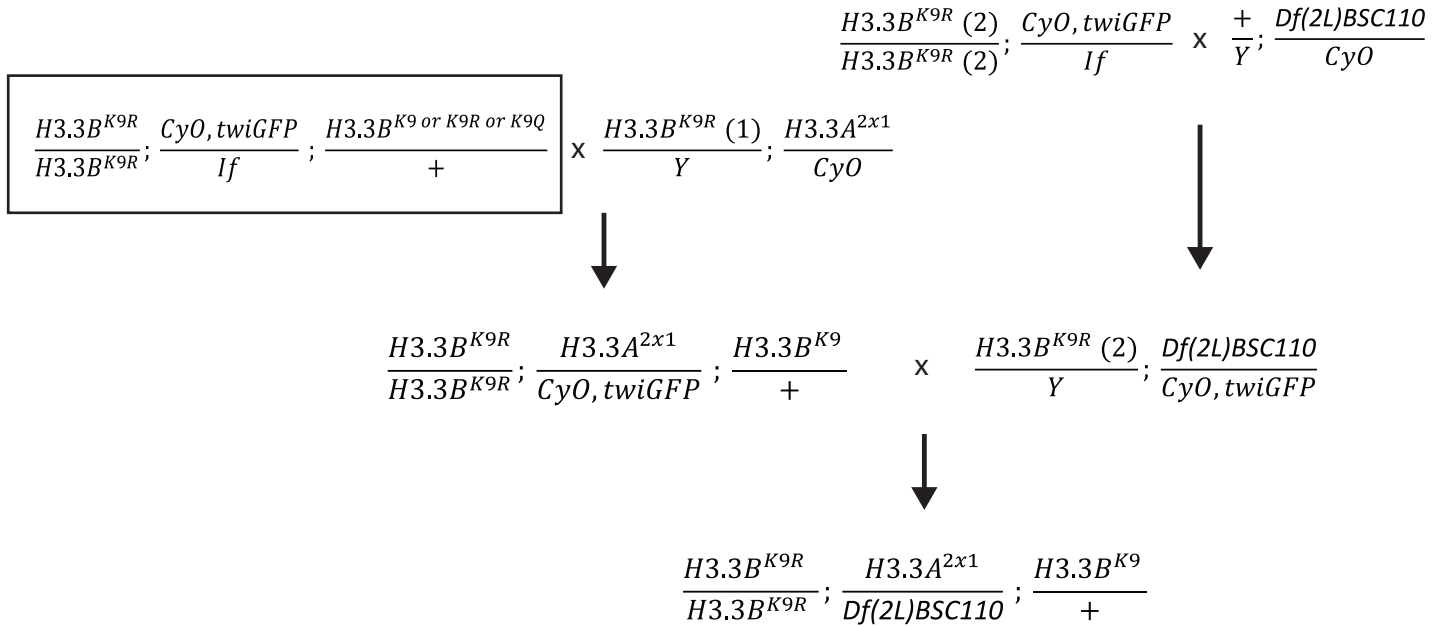


$$\frac{H3.3B^{K9R} (1)}{H3.3B^{K9R} (2)}; \frac{H3.3A^{2x1}, His\Delta, twiGal4}{H3.3A^{2x1}, His\Delta, UAS2xYFP}; \frac{12x H3^{HWT} \text{ or } 12x H3^{K9R}}{+}$$

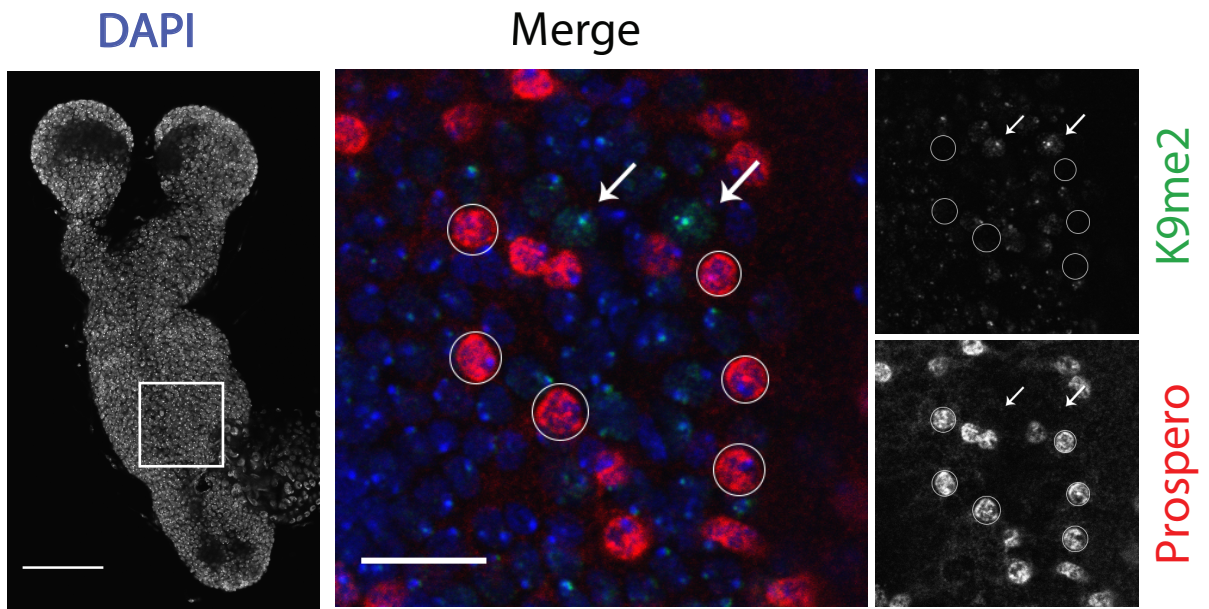
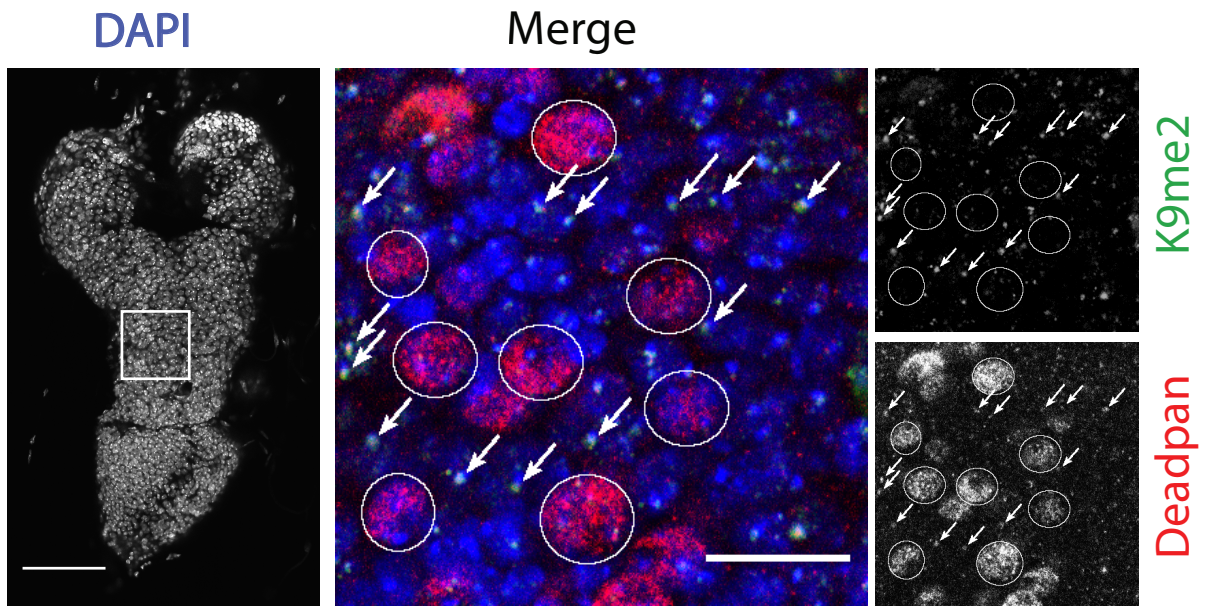
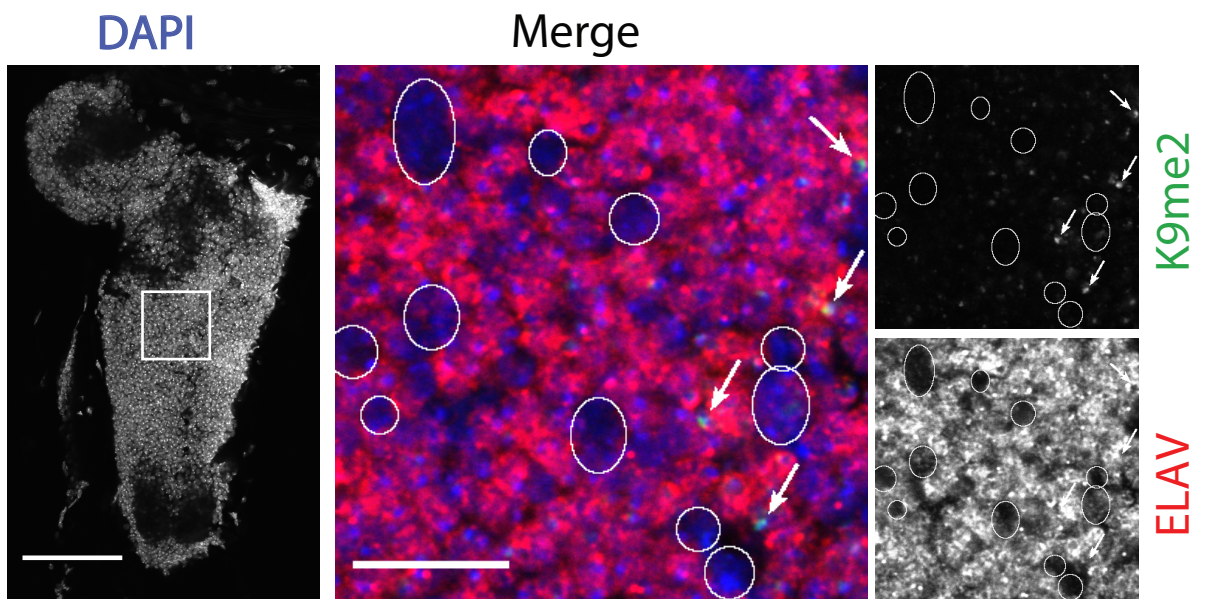
$H3^{HWT} = \frac{+}{+}; \frac{His\Delta, twiGal4}{His\Delta, UAS2xYFP}; \frac{12x H3^{HWT}}{+}$
$H3^{K9R} = \frac{+}{+}; \frac{His\Delta, twiGal4}{His\Delta, UAS2xYFP}; \frac{12x H3^{K9R}}{+}$
$H3.3^{K9R} H3^{HWT} = \frac{H3.3B^{K9R}}{H3.3B^{K9R}}; \frac{H3.3A^{2x1}, His\Delta, twiGal4}{H3.3A^{2x1}, His\Delta, UAS2xYFP}; \frac{12x H3^{HWT}}{+}$
$H3.3^{K9R} H3^{K9R} = \frac{H3.3B^{K9R}}{H3.3B^{K9R}}; \frac{H3.3A^{2x1}, His\Delta, twiGal4}{H3.3A^{2x1}, His\Delta, UAS2xYFP}; \frac{12x H3^{K9R}}{+}$

**Supplementary Figure 1: Crossing scheme to generate *H3.3<sup>K9R</sup>* mutants and *H3.3<sup>K9R</sup> H3<sup>K9R</sup>* double mutants.** A) Diagram of crosses used to generate *H3.3<sup>K9R</sup>* mutants. B) Diagram of crosses used to generate *H3.3<sup>K9R</sup> H3<sup>K9R</sup>* combined mutants. Stocks of intermediate genotypes could not be maintained. *H3.3B<sup>K9R</sup>* 1 and 2 refer to independent CRISPR-Cas9-mediated substitution events. Df-H3.3A refers to deficiency uncovering H3.3A (Df(2L)BSC110). Boxed insets delineate full genotype for shorthand of all mutant flies used. All genotypes were confirmed through high-throughput sequencing data.

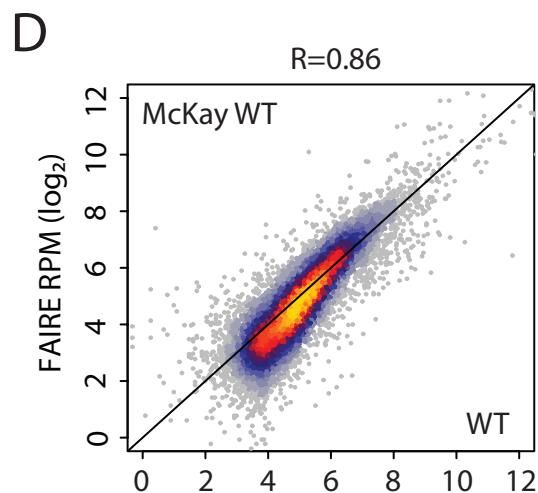
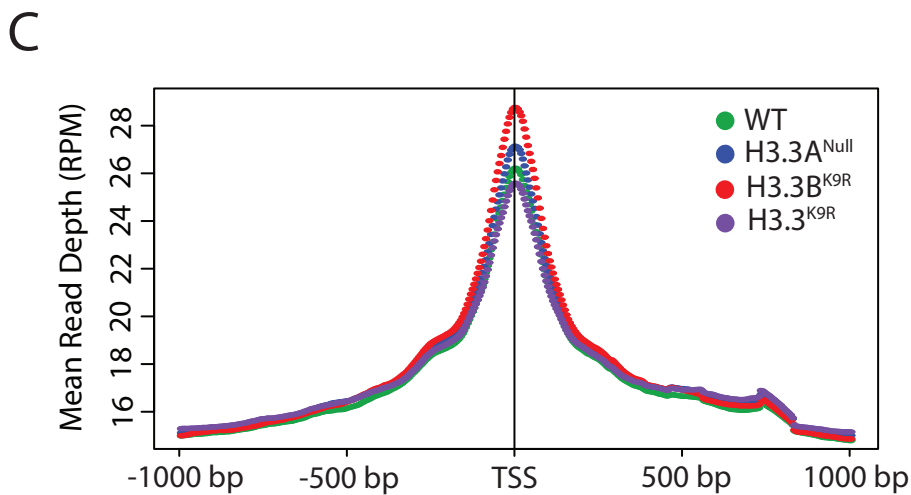
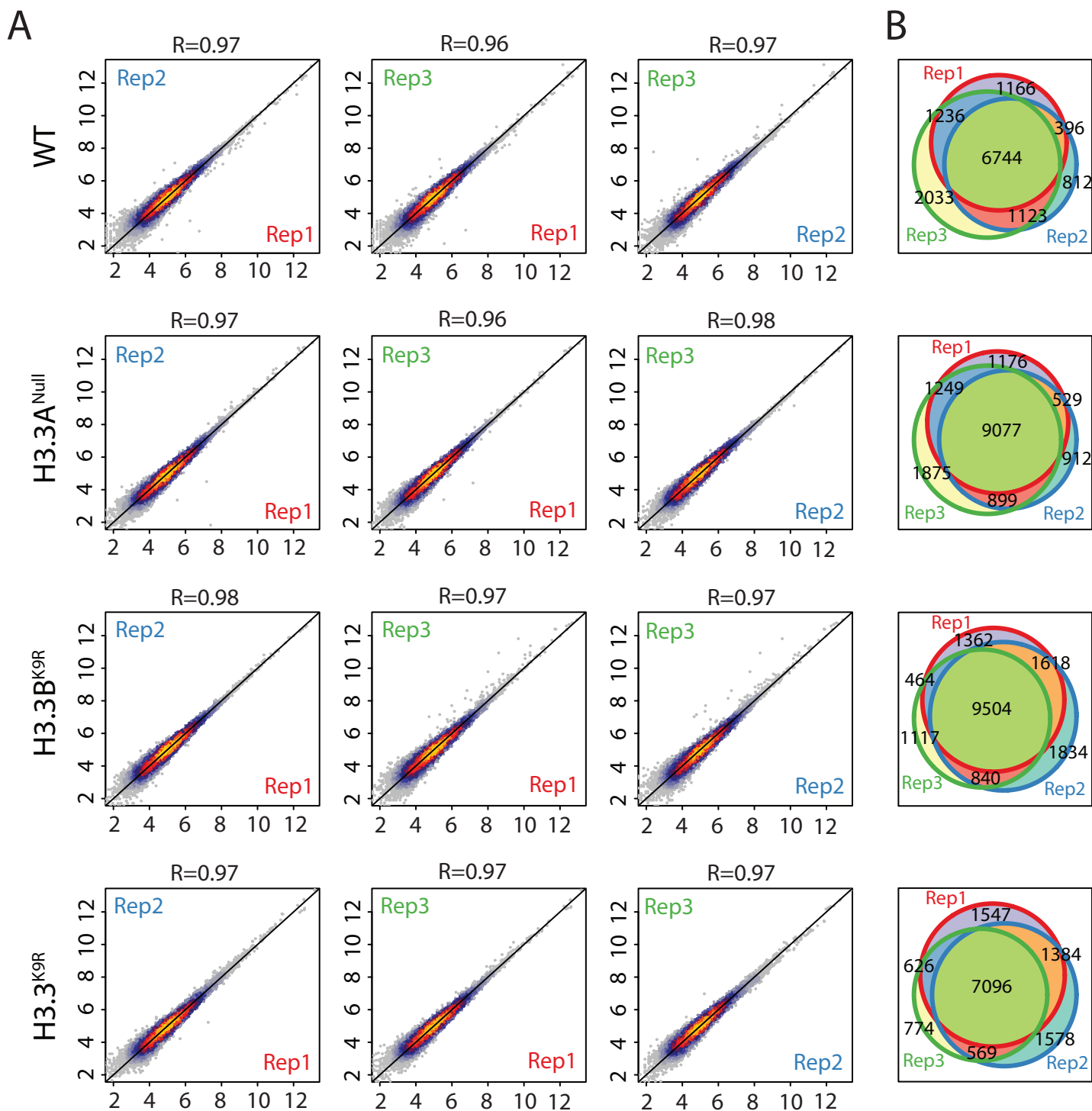
A



**Supplementary Figure 2: Crossing scheme to generate *H3.3<sup>K9R</sup>* mutants with H3.3B ectopically expressed transgenes.** A) Diagram of crosses used to generate *H3.3<sup>K9R</sup>* mutants with H3.3B<sup>K9</sup>, H3.3B<sup>K9R</sup>, or H3.3B<sup>K9Q</sup> transgene. Box indicates fly genotype that was sterile in H3.3B<sup>K9R</sup> and H3.3B<sup>K9Q</sup> expressing animals.

**A****B****C**

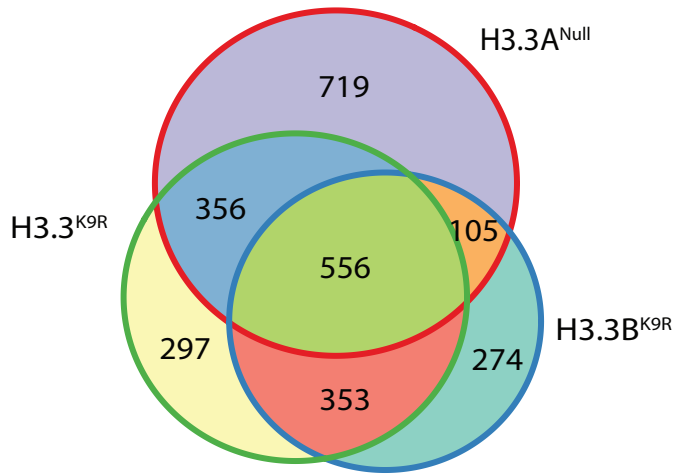
**Supplementary Figure 3: Residual H3K9me2 signal is found in differentiated neurons in *H3<sup>K9R</sup>* mutants.** *H3<sup>K9R</sup>* 1st instar brains were stained with DAPI in blue, anti-K9me2 in green, and either anti-Prospero (A), anti-Deadpan (B), or anti-ELAV (C) in red. Prospero marks ganglion mother cells, deadpan marks neuroblasts, and ELAV marks differentiated neurons. Arrows indicate K9me2 positive cells in which signal overlaps the chromocenter. Circles in A and B indicate prospero or deadpan positive cells respectively whereas circles in C indicate ELAV negative cells. K9me2 positive cells contain ELAV but neither prospero or deadpan. Single slice images of the whole brain are shown in the left panel (scale bar = 50 microns) and magnified views (white box) of individual cells are shown in the right panels (scale bar = 10 microns).



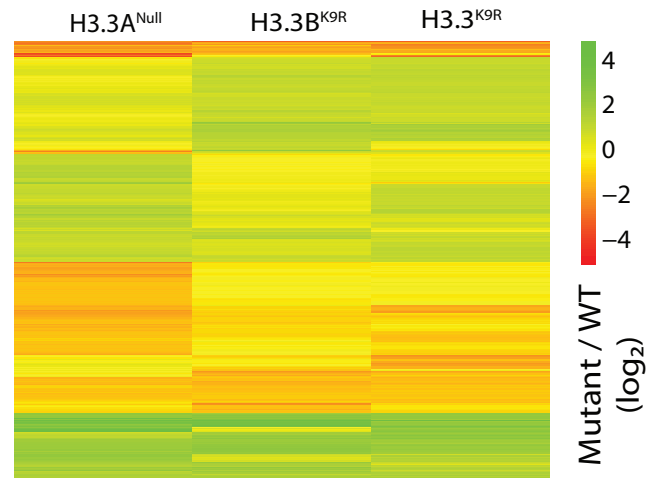
**Supplementary Figure 4: Imaginal wing disc FAIRE signal is highly consistent across replicates and with previously generated FAIRE data.** A) Scatterplots comparing normalized FAIRE signal at merged set of FAIRE peaks for all replicates of a particular genotype. Signal expressed as log<sub>2</sub> reads per million (RPM). R value indicates Pearson Correlation. B) Venn Diagram showing overlap of MACS2 called peaks demonstrates peaks were highly similar across replicates. C) Average FAIRE signal at 5bp bins surrounding transcription start sites (TSS). Signal expressed as average reads per million (RPM). D) Correlation analysis of FAIRE signal at merged set of FAIRE peaks from average WT and previously published FAIRE data in wing discs (McKay & Lieb 2013).



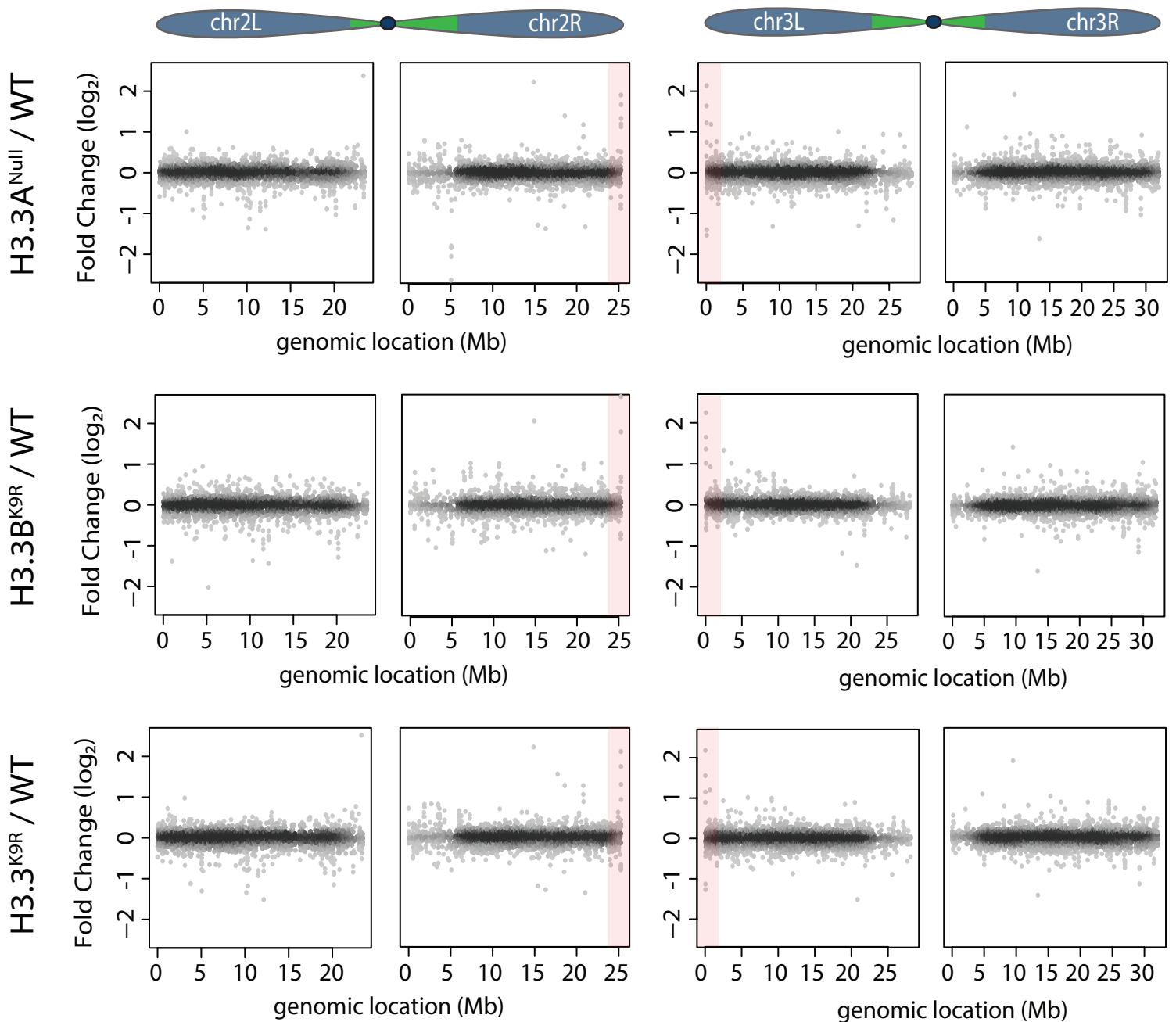
A



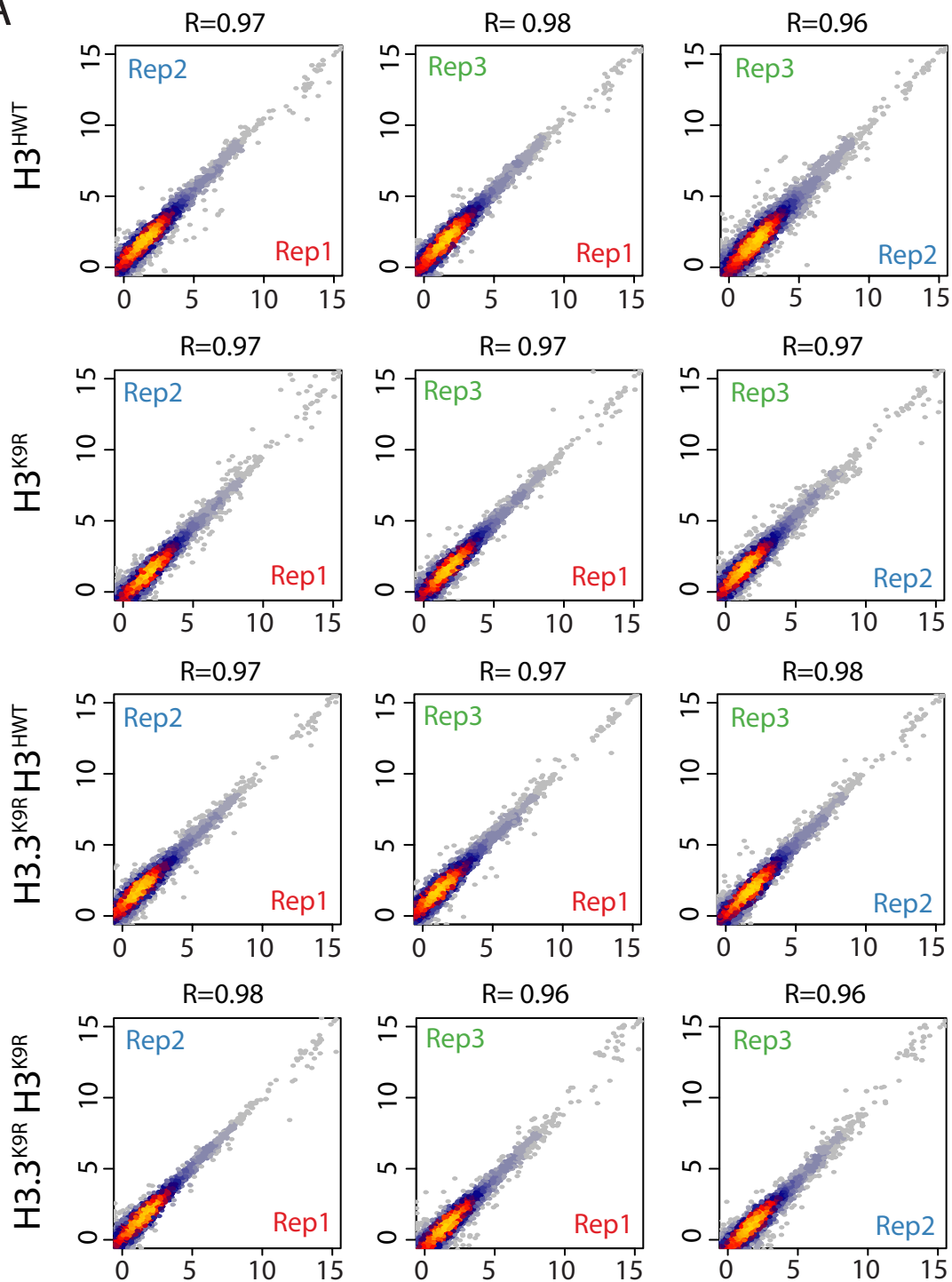
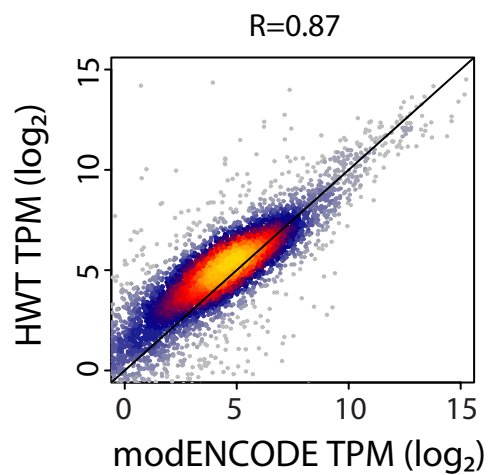
B



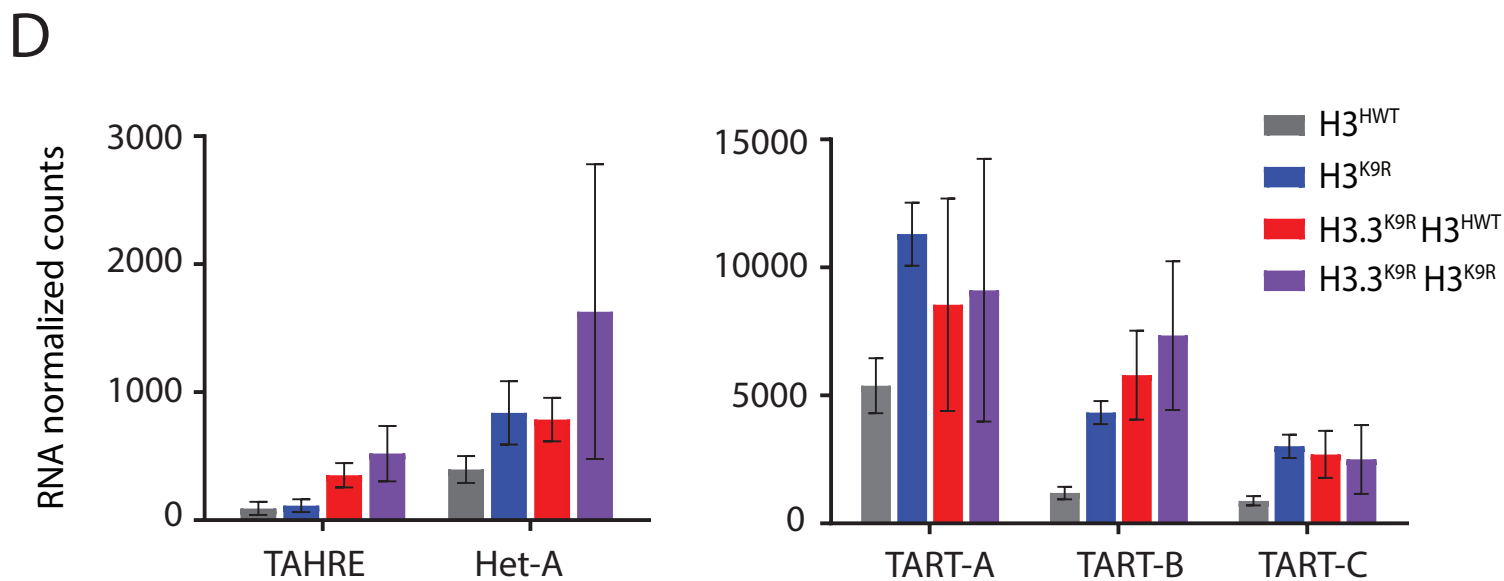
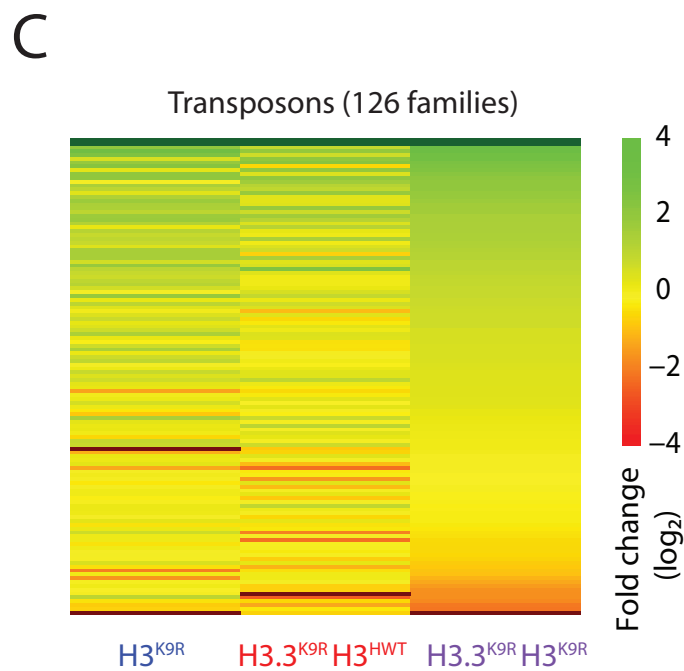
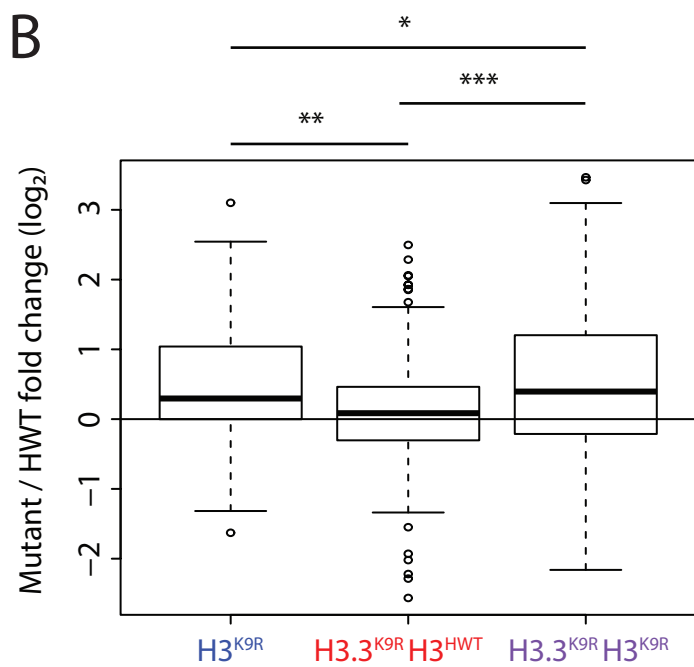
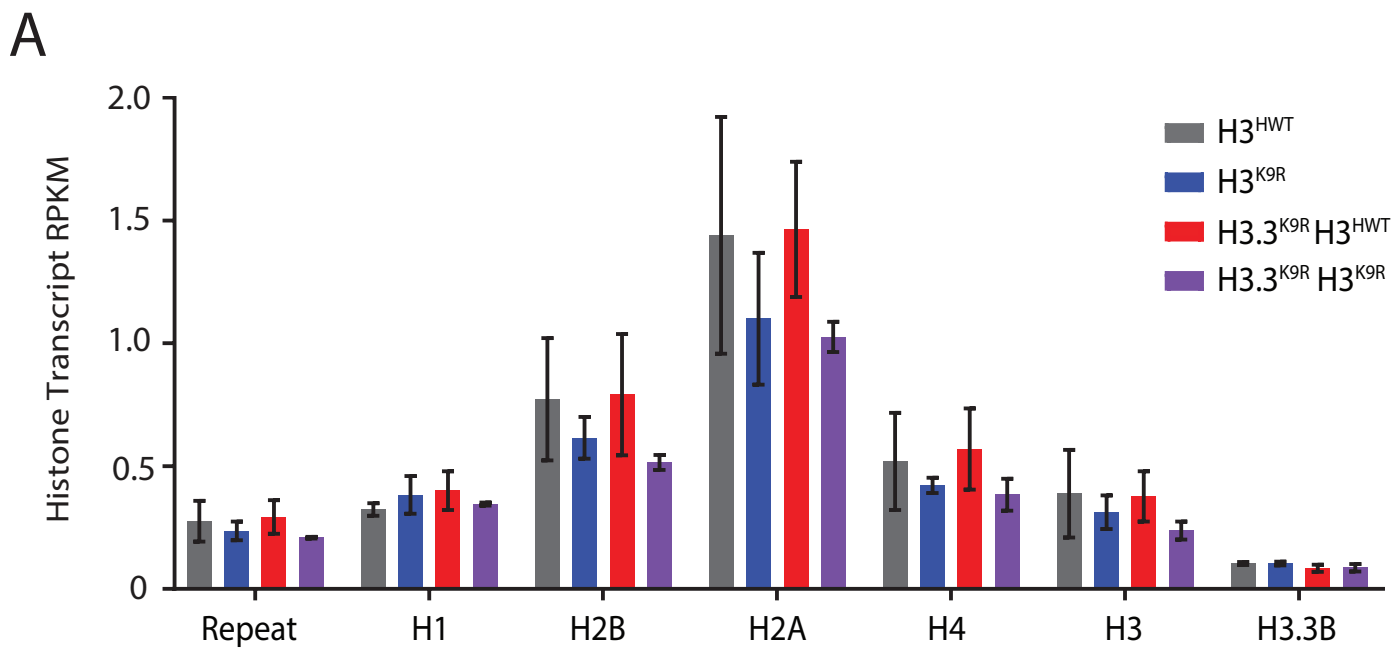
C



**Supplementary Figure 5: Regions of significantly changed FAIRE signal are similar across H3.3 mutants.** A) Venn diagram showing overlap of FAIRE peaks with significantly changed FAIRE signal between H3.3 mutant and WT samples. Significance cutoff set at adjusted p value of 0.05 as determined by DESeq2 package (Love et al. 2015). B) Heatmap showing H3.3 mutant over WT fold change ( $\log_2$ ) of FAIRE signal at all significantly different FAIRE peaks shown in A. Fold changes are not exacerbated in *H3.3<sup>K9R</sup>* double mutants compared to either *H3.3B<sup>K9R</sup>* or *H3.3A* single mutant alone. C) Ratio of H3.3 mutant over WT FAIRE signal plotted versus genome coordinate of FAIRE peaks on chromosome 2 and 3. Light red boxes highlight telomeric areas with changes in FAIRE signal. Blue areas of the chromosome diagram indicate largely euchromatic regions, and green areas of the chromosome diagram represent approximate locations of pericentromeric heterochromatin (Hoskins et al. 2015; Riddle et al. 2011). Mb = megabase.

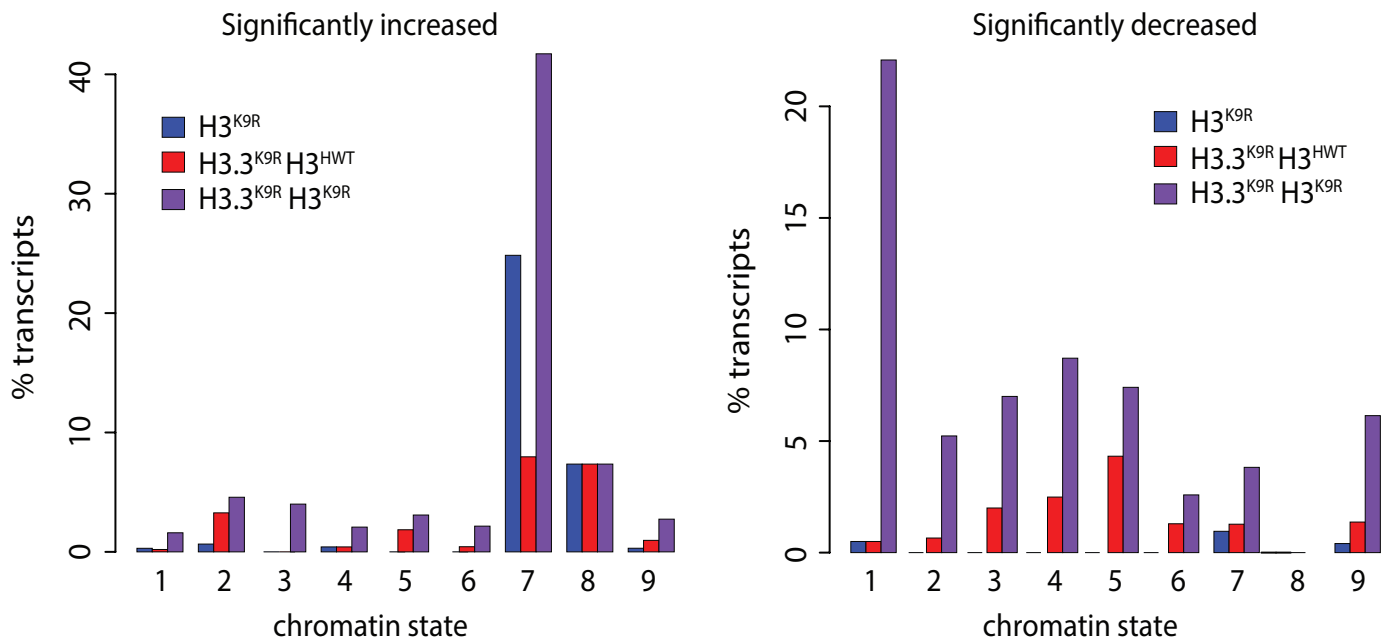
**A****B**

**Supplementary Figure 6: 1st instar larvae RNA signal of  $H3.3^{K9R}$  and  $H3^{K9R}$  mutants is highly consistent across replicates and with previously generated RNA data.** A) Scatterplot of normalized RNA signal at transcripts assembled by cufflinks for all replicates of a particular genotype. RNA signal shown in log2 transformed transcripts per million (TPM). R indicates Pearson correlation. B) Scatterplot of normalized RNA signal comparing  $H3^{HWT}$  and modENCODE RNA-seq data for 1st instar larvae (Graveley et al. 2011).



**Supplementary Figure 7: RNA signal across transposon families is increased in *H3.3<sup>K9R</sup>* and *H3<sup>K9R</sup>* mutants.** A) Histone steady-state RNA levels are similar between variant and canonical K9R mutants. Reads were mapped using Bowtie2 to a custom index file containing one copy of the histone repeat (one copy of each replication-dependent histone) and H3.3B. Shown are the RPKM values in the coding region of each individual histone or across the entire histone repeat. Reads were normalized to the number of reads that uniquely map to the entire genome. Error bars represent standard deviation of three independent replicates for each genotype. B-D) Normalized counts of RNA signal at transposon families determined by piPipes pipeline (Han et al. 2015). B) Boxplot showing average fold change of RNA signal at 126 transposon families in *H3.3<sup>K9R</sup>* and *H3<sup>K9R</sup>* mutants compared to *H3<sup>HWT</sup>*. Paired t-tests were used to analyze statistical differences across genotypes (\*  $p < 0.05$ , \*\*  $p < 0.005$ , \*\*\*  $p < 0.0005$ ). C) Heatmap of FAIRE signal showing K9R mutants over *H3<sup>HWT</sup>* fold change at transposon families. D) Average RNA normalized counts at telomeric transposons in K9R mutants. Error bars indicate standard deviation derived from three replicates for each genotype.

A



**Supplementary Figure 8: H3.3K9 compensates for H3K9 at regions of H3K9ac and partially at regions of H3K9me.** A) Barplot similar to Figures 7A and 7B showing the percent of transcripts in each chromatin state that are significantly changed in a K9R mutant compared to  $H3^{HWT}$ . In contrast to Figure 7, only those transcripts that overlap a single chromatin state are shown, demonstrating that the majority of transcripts that decrease in  $H3.3^{K9R} H3^{K9R}$  mutants compared to  $H3^{HWT}$  are in chromatin state 1 (regions of H3K9ac and H3K4me).